Published in final edited form as:
Chronobiol Int. 2012 July ; 29(6): 653–664. doi:10.3109/07420528.2012.679330.

Fibroblast Circadian Rhythms of PER2 Expression Depend on Membrane Potential and Intracellular Calcium

Takako Noguchi[1], **Connie W. Wang**[1], **Haiyun Pan**[1,2], and **David K. Welsh**[1,2]

Takako Noguchi: tnoguchi@ucsd.edu; Connie W. Wang: cwang08@gmail.com; Haiyun Pan: orchid105@gmail.com; David K. Welsh: welshdk@ucsd.edu

[1]Department of Psychiatry and Center for Chronobiology, University of California, San Diego, 9500 Gilman Drive MC0603, La Jolla, CA 92093-0603, USA

[2]Veterans Affairs San Diego Healthcare System, 3350 La Jolla Village Drive, San Diego, CA 92161, USA

Abstract

The suprachiasmatic nucleus (SCN) of the hypothalamus synchronizes circadian rhythms of cells and tissues throughout the body. In SCN neurons, rhythms of clock gene expression are suppressed by manipulations that hyperpolarize the plasma membrane or lower intracellular Ca^{2+}. However, whether clocks in other cells also depend on membrane potential and calcium is unknown. In this study, we investigate the effects of membrane potential and intracellular calcium on circadian rhythms in mouse primary fibroblasts. Rhythms of clock gene expression were monitored using a PER2::LUC knockin reporter. We found that rhythms were lost or delayed at lower (hyperpolarizing) K^+ concentrations. Bioluminescence imaging revealed that this loss of rhythmicity in cultures was due to loss of rhythmicity of single cells rather than desynchrony among cells. In lower Ca^{2+} concentrations, rhythms were advanced or had shorter periods. Buffering intracellular Ca^{2+} by the calcium chelator 1,2-Bis(2-aminophenoxy) ethane-N,N,N′,N′-tetraacetic acid tetrakis acetoxymethyl ester (BAPTA-AM) or manipulation of IP_3-sensitive intracellular calcium stores by thapsigargin delayed rhythms. These results suggest that the circadian clock in fibroblasts, as in SCN neurons, is regulated by membrane potential and Ca^{2+}. Changes in intracellular Ca^{2+} may mediate the effects of membrane potential that we observed.

INTRODUCTION

In mammals, circadian rhythms of physiology and behavior depend on a master biological clock located in the brain, in the suprachiasmatic nucleus (SCN), which is required to synchronize cellular clocks throughout the body (Mohawk & Takahashi, 2011; Welsh et al., 2010). The master SCN pacemaker is synchronized to the day/night cycle by light input from the retina, and in turn generates rhythmic neuronal signals to synchronize other cells outside the SCN. A transcription-translation negative feedback loop underlies circadian oscillations in SCN and other cells. This core loop involves activation of *Period* (*Per1, Per2, Per3*) and *Cryptochrome* (*Cry1* and *Cry2*) gene transcription by a *Bmal1/Clock* heterodimer and delayed inhibition of this process by complexes containing PER and CRY proteins (Mohawk et al., 2011).

Correspondence to: David K. Welsh, welshdk@ucsd.edu.

Declaration of Interest: The authors report no conflicts of interest. The authors alone are responsible for the content and writing of the paper.

In the SCN, many components of cell signaling, such as intracellular Ca^{2+} ($[Ca^{2+}]_i$) (Ikeda et al., 2003), cAMP (O'Neill et al., 2008), membrane potential (Kuhlman & McMahon, 2004), neuronal firing (Nakamura et al., 2008; Welsh et al., 1995), and neurotransmitter release (M. Hastings et al., 2007) oscillate in a circadian manner. Recent work indicates that some of these non-transcriptional rhythmic processes may be necessary to maintain clock function. For example, membrane hyperpolarization in rat SCN slice cultures, achieved by lowering extracellular potassium ($[K^+]_o$), reversibly abolishes rhythmic expression of *Per1* (Lundkvist et al., 2005). Lowering extracellular calcium ($[Ca^{2+}]_o$) also abolishes rhythmic expression of *Per1*, not only in SCN slices but also in liver explants (Lundkvist et al., 2005). Modulating $[Ca^{2+}]_i$ by ryanodine, a blocker of certain intracellular Ca^{2+} stores, alters neuronal firing and $[Ca^{2+}]_i$ rhythms in mouse SCN neurons (Ikeda et al., 2003). In *Drosophila*, silencing of electrical activity leads to loss of rhythmic expression of the PERIOD and TIMELESS proteins, core constituents of the fly circadian clock (Nitabach et al., 2002). Furthermore, buffering $[Ca^{2+}]_i$ in *Drosophila* pacemaker neurons, by expressing the genetically encoded calcium buffer parvalbumin, results in dose-dependent slowing of free-running behavioral rhythms (Harrisingh et al., 2007). These data suggest that membrane potential or neuronal firing and underlying ionic fluxes may play a central role in rhythm generation in pacemaker neurons. However, it is not yet clear whether this applies more generally to circadian clocks in peripheral tissues.

Resting membrane potentials and basic properties of ion channels in fibroblasts have been studied. Resting potentials of fibroblasts are mainly determined by K^+ currents; increasing $[K^+]_o$ depolarizes and decreasing $[K^+]_o$ hyperpolarizes membrane potential of fibroblasts just as in SCN neurons (Baxter et al., 2002; Bouskila & Dudek, 1995; Chilton et al., 2005; Lundkvist et al., 2005; Yen-Chow et al., 1984).

Here, we show that membrane potential and Ca^{2+} signaling are critical for molecular rhythmicity within mammalian fibroblasts. We used knockin mice that express a fusion protein incorporating PER2 and firefly luciferase (PER2::LUC) to assay real-time clock gene expression in fibroblast cultures. Membrane hyperpolarization caused by reducing $[K^+]_o$ abolished PER2::LUC rhythms in fibroblasts. Reducing $[Ca^{2+}]_o$ or $[K^+]_o$, or modulating intracellular Ca^{2+} stores pharmacologically, also affected the phase and period of PER2::LUC rhythms in fibroblasts.

MATERIALS AND METHODS

Animals

Generation of $mPer2^{Luciferase}$ (PER2::LUC) knockin mice was described previously (Yoo et al., 2004). For this study, we used an alternative PER2::LUC mouse line incorporating an SV40 polyadenylation site to enhance expression levels (Welsh et al., 2004). The mice were developed at Northwestern University using the same methodology as the original strain of knockin mice (Yoo et al., 2004). Mice were bred as homozygotes and maintained in LD 12:12 light cycles (12 hr light, 12 hr dark) throughout gestation and from birth until used for experiments. Mouse studies were conducted in accordance with regulations of the Committee on Animal Care and Use at University of California, San Diego. The experimental protocols conform to international ethical standards (Portaluppi et al., 2010).

Cell and Explant Culture

Primary fibroblasts and SCN slices were prepared from neonatal (1–7 day old) PER2::LUC knockin mice. Fibroblasts were dissociated from tails by incubation in trypsin, with mild mechanical agitation followed by trituration. Fibroblasts were plated in 35 mm culture dishes and cultured in medium consisting of bicarbonate-buffered DMEM (GIBCO

11995-065), supplemented with 25 U/ml penicillin, 25 μg/ml streptomycin, and 10% fetal bovineserum (GIBCO 26140-079), and maintained in a standard tissue culture incubator at 37°C, equilibrated with 5% CO_2. For experiments, 35 mm culture dishes with confluent fibroblasts were covered by 40 mm circular coverslips (Erie Scientific 40CIR1), sealed in placewith vacuum grease to prevent evaporation. SCN slices were cut by tissue chopper (Stoelting, Wood Dale, U.S.A.) to a thickness of 250 μm and cultured on Millicell-CM membrane inserts (Millipore PICMORG50). SCN slices were cultured in HEPES-buffered, air-equilibrated "Home Made Medium" (HMM) [pH 7.4; serum-free, 350 mg/l sodium bicarbonate, no phenol red; made by mixing MEM Vitamin solution [GIBCO 11120-052], MEM amino acid solution [GIBCO 11130-051], and other individual components according to the formulation of DMEM (Invitrogen 12100046), supplemented with 10 mM HEPES, 25 U/ml penicillin, 25 μg/ml streptomycin, 2% B-27 (GIBCO 17504-044), and 1 mM luciferin potassium salt (BioSynth L-8220), or 1 mM luciferin sodium salt (BioSynth L-8240)]. For luminescencerecordings, fibroblasts and SCN slices were transferred to HMM with specific concentrations of K^+ and Ca^{2+}. Formulations of HMM with various concentrations of K^+ and Ca^{2+} are listed in Table 1.

Ryanodine (Alexix biochemicals, Lausen, Switzerland), nimodipine (MP biomedicals, Solon, OH), BAPTA-AM (Sigma), and thapsigargin (Sigma) were dissolved in DMSO (Sigma). EGTA (ethylene glycol tetraacetic acid) (Sigma) was dissolved in dH_2O. These drugs were added in concentrations that do not damage fibroblasts over 7 days. Adding greater than 50 μM BAPTA-AM, 100 nM thapsigargin, 8 μM nimodipine, or 20 μM EGTA damaged fibroblasts irreversibly (data not shown). Final concentration of DMSO in medium was 0.1%.

Luminometry

For measuring luminescence rhythms from cultures, we placed the sealed 35 mm culture dishes into a luminometer (LumiCycle, Actimetrics, Inc., Wilmette, IL), inside a standard tissue culture incubator kept at 36°C, dry, 0% CO_2. Luminescence from each dish was measured by a photomultiplier tube for 70 s at intervals of 10 min and recorded as counts/sec for > 7 days. Due to high initial transients of luminescence after medium change, the first 12 h of data were excluded from analysis. The first 24 h of data was removed from amplitude analysis for experiments using Ca^{2+} modulating drugs because of acute responses to drugs. When the average bioluminescence intensity was less than 70 counts/sec over 7 days or dropped to background level (20–50 counts/sec) within 4 days, the cells were considered damaged, and excluded from analysis. A 24 h running average baseline was subtracted from the raw data.

Bioluminescence Imaging

Before single-cell imaging, PER2::LUC fibroblasts were cultured for at least 2 weeks in explant medium [DMEM (Invitrogen 12100046), serum-free, 1.2 g/L sodium bicarbonate, with phenol red, pH 7.4], supplemented with 10 mM HEPES, 25 U/ml penicillin, 25 μg/ml streptomycin, and 2% B-27 (GIBCO 17504-044). In some samples, 1–5% PER2::LUCfibroblasts were mixed with non-luminescent wild type (C57/BL6J) fibroblasts to facilitate identification and tracking of single cells. For imaging, explant medium was replaced with HMM. The imaging was performed as previously described (Welsh et al., 2005; Welsh & Noguchi, 2011). Briefly, the culture was placed on the stage of an inverted microscope (Olympus IX71, Tokyo, Japan). A heated lucite chamber custom-engineered to fit around the microscope stage (Solent Scientific, Segensworth, UK) kept the cells at a constant 36°C. The microscope rested on an anti-vibration table (TMC, Peabody, MA) in a dark, windowless room, isolated by black curtains. After focusing carefully with bright-field illumination, we eliminated stray light by covering the dish with a small black lucite box,

draping the microscope with opaque black plastic sheeting (Thorlabs BK5, Newton, NJ), and darkening the room completely. Light from the sample was collected by an Olympus 4x XLFLUOR objective (NA 0.28) and transmitted directly to a cooled CCD camera mounted on the bottom port of the microscope. We used the "Series 800" camera made by Spectral Instruments (Tucson, AZ), containing a back-thinned CCD thermoelectrically cooled to −90°C with a rated quantum efficiency of 92% at 560 nm. We measured read noise of 2.5 electrons at 50 KHz readout and dark current of 0.0002 electrons/pixel/sec. The signal-to-noise ratio was increased by 8 × 8 binning of the 1056 × 1032 pixel array. Images were typically collected at intervals of 30 min, with 29.5 min exposure duration. Images were acquired to computer using SI Image SGL D software (Spectral Instruments), saved to hard disk, and analyzed with MetaMorph (Universal Imaging Corp., Buckinghamshire, UK).

Image Processing

In MetaMorph, cosmic ray artifacts were removed by pixel-wise comparison of pairs of consecutive images, i.e. using the minimum value of each pixel to construct a new image from every pair of consecutive images. Thus, data were effectively smoothed by a running minimum algorithm, with a temporal window twice the duration of a single exposure (i.e., a smoothing window of 60 min for 30 min exposures). In the resulting stack of images, luminescence intensity was measured within a region of interest defined manually for each cell. The position of the region was adjusted if necessary to accommodate movements of cells during the experiment, but its size was kept constant across the time series. Data were logged to Microsoft Excel files for plotting and further analysis. Luminescence intensity values were corrected for bias and dark current by subtracting the minimum intensity of a background region devoid of cells, and converted to photons/min based on the rated quantum efficiency and gain of the camera.

For raster plots, bioluminescence-intensity data were aligned by the peak 0.5 – 2 d after recording. Using Gene Cluster 3.0 and Treeview (developed by Dr. Michael Eisen while at Stanford University), data were detrended by subtracting an average value, normalized so that the sum of the squares of the values is 1.0, then color coded, with white for positive and black for negative values.

Rhythm Data Analysis

Overall brightness was calculated by averaging values from 0.5 d after start of recording to the end of recording. For luminometry data, brightness values were normalized across treatment conditions using a control sample run in parallel. Circadian rhythmicity was assessed by spectral analysis using the FFT algorithm in LumiCycle Analysis (Actimetrics). Cells were considered to show significant circadian rhythmicity when at least 6% of total spectral power (in the period range 0–36h) was contributed by the highest point in the circadian range (20–36 h), similar to methods described previously (Ko et al., 2010; Liu et al., 2007). For samples categorized as rhythmic by spectral analysis, we computed rhythm parameters using LumiCycle Analysis (Actimetrics). To obtain period, phase, and amplitude, data were fitted to a sine wave with exponentially decaying amplitude. For luminometry data, amplitudes were normalized to amplitude and relative brightness of control samples run in parallel. For imaging data, amplitudes were normalized to brightness of the cell and control. Phase shifts were calculated by comparing peaks ~2.5 days after medium change to control samples run in parallel. For cell counts, cells were trypsinized 2 days after medium change, and numbers of cells were normalized to control samples run in parallel. Differences from control values were assessed by Student's t-test, Mann-Whitney U-test, or ANOVA followed by Dunnett's test.

RESULTS

Manipulations of $[K^+]_o$,$[Ca^{2+}]_o$, and $[Ca^{2+}]_i$ abolish circadian rhythms of SCN slices

To confirm the effects of $[K^+]_o$, $[Ca^{2+}]_o$, and $[Ca^{2+}]_i$ manipulation on SCN neurons, we cultured SCN slices in HMM with lower $[K^+]_o$ and $[Ca^{2+}]_o$. We also added BAPTA-AM (a membrane permeable Ca^{2+} chelator) to reduce $[Ca^{2+}]_i$. SCN slices were cultured in HMM control (6.3 mM K^+ and 1.8 mM Ca^{2+}) for 1–2 weeks and then cultured in testing medium for 6–7 days. As shown in a previous report (Lundkvist et al., 2005), decreasing $[K^+]_o$, decreasing $[Ca^{2+}]_o$, or adding BAPTA-AM greatly reduced the amplitude of circadian rhythms of SCN slices. Representative recordings at 1 mM K^+, 0 mM Ca^{2+}, and 40 μM BAPTA-AM are shown in Figure 1.

Decreasing $[K^+]_o$ abolishes PER2::LUC oscillations in fibroblast cultures

Resting membrane potential in cells depends on the K^+ ion gradient across the plasma membrane. Decreasing $[K^+]_o$ hyperpolarizes and increasing $[K^+]_o$ depolarizes fibroblasts (Chilton et al., 2005; Yen-Chow et al., 1984). To test whether hyperpolarizing the fibroblast membrane affects clock gene oscillations in fibroblasts as it does in SCN neurons (Lundkvist et al., 2005), we cultured fibroblasts from PER2::LUC mice in HMM medium containing 0, 0.2, 0.4, 1, 1.7, 3.6, 6.3, 12, 22, and 44 mM K^+. Bioluminescence recording was started just after changing from standard DMEM to test media. We normalized results to values obtained for medium with 6.3 mM K^+ (HMM control), which is the closest to standard DMEM (5.3 mM).

At 1–44 mM K^+, all fibroblast cultures showed clear circadian rhythms (Fig. 2D–F), and there were no significant differences in any of the parameters measured (average brightness, % rhythmic samples, amplitude, period, or phase), except for increased amplitude at 44 mM K^+ (Fig. 2G–K). In the absence of K^+, however, only 1 out of 9 samples (11%) was rhythmic by spectral analysis. Average brightness was not significantly affected. At 0.2 mM K^+, 2 out of 6 samples (33%) were rhythmic by spectral analysis, but they showed higher average brightness relative to 6.3 mM K^+ control [$p < 0.01$, *ANOVA* followed by Dunnett's test]. At 0 and 0.2 mM K^+, circadian parameters (amplitudes, periods and phases) could not be statistically analyzed because samples were mostly arrhythmic (Fig. 2G–K). At 0.4 mM K^+, 88% of samples (7 out of 8 samples) were rhythmic by spectral analysis. They showed higher average brightness, and delayed phases relative to 6.3 mM K^+ control [$p < 0.01$, *ANOVA* followed by Dunnett's test] (Fig. 2G–K).

Culturing fibroblasts in HMM with 0 – 22 mM K^+ did not significantly affect cell viability (Fig. 2L). Fibroblasts cultured in HMM with 0 mM K^+ could recover rhythmic PER2::LUC expression after changing medium to HMM control (Fig. 3). The amplitudes of samples recovered after 0 mM K^+ was 2.9 times greater than for HMM control (n = 3 each, $p < 0.05$; Mann-Whitney *U*-test).

Decreasing $[K^+]_o$ abolishes PER2::LUC oscillations in single fibroblasts

Under constant conditions in vitro, rhythms of fibroblast cultures or peripheral tissue explants damp partially or completely. This is caused by loss of synchrony among individual cells (Nagoshi et al., 2004; Welsh et al., 2004), but single cell amplitude can also vary (Pulivarthy et al., 2007). To determine whether decreasing $[K^+]_o$ caused desynchrony or reduction in amplitude of individual oscillators, we studied single-cell circadian oscillations by PER2::LUC imaging. A total of 53 fibroblasts from 5 cultures in control HMM and 44 cells from 3 cultures in 0 mM K^+ HMM were monitored for 6–7 d. For analysis, we chose cells that did not move extensively and could be followed for the entire 6–7 d experiment. In 0 mM K^+ HMM, although the results were not statistically significant [p > 0.05, Student's *t*-

test], brightness of single cells decreased by 20% compared to control HMM (Fig. 4C), consistent with luminometry results (Fig. 2G). About 77% of cells were rhythmic in control HMM (Fig. 4A, D), whereas only 16% of cells were rhythmic in 0 mM K^+ HMM (Fig. 4B, D). Reflecting the poor rhythmicity, average single cell amplitudes in 0 mM K^+ HMM were decreased to 57% of control [$p < 0.01$, Student's *t*-test] (Fig. 4E). In 0 mM K^+ HMM, cells that were rhythmic had similar circadian periods (24.7 ± 0.7 h, mean ± SE) relative to cells in control HMM (25.0 ± 0.3 h) (Fig. 4F). Bioluminescence patterns of all single cells cultured either in control HMM or 0 mM K^+ HMM are illustrated in raster plot format, sorted by phase of the peak at 0.5 – 2 d after start of recording (Fig. 4G–H). Persistent rhythms are observed for fibroblasts cultured in control HMM but not for fibroblasts cultured in 0 mM K^+ HMM. Thus, loss of rhythmicity observed by luminometry in fibroblast cultures at 0 mM K^+ HMM is explained by loss of rhythmicity or reduced amplitude of single cells.

Decreasing $[Ca^{2+}]_o$ shortens circadian periods of fibroblasts

Depolarization caused by high $[K^+]_o$ in mammalian fibroblasts induces influx of Ca^{2+} (Etcheberrigaray et al., 1993; Gee et al., 2000). Therefore, we next addressed the question of whether preventing Ca^{2+} influx by removing $[Ca^{2+}]_o$ has an effect on fibroblast PER2::LUC rhythms similar to that of hyperpolarizing the cells with low $[K^+]_o$. We cultured fibroblasts in HMM containing 0, 0.23, 0.45, 0.9, 1.8, 3.6, 7.2, or 14.4 mM Ca^{2+}, or 10 μM EGTA in 0 mM Ca^{2+} HMM. Results were compared to HMM control medium containing 6.3 mM K^+ and 1.8 mM Ca^{2+}. Unlike for manipulations of $[K^+]_o$, the cyclic expression of PER2 was not reduced or abolished in medium containing lower or higher $[Ca^{2+}]_o$ (Fig. 5A). All samples, except for one sample in 3.6 mM Ca^{2+}, were categorized as rhythmic by spectral analysis. Brightness was lower at lower $[Ca^{2+}]_o$ and higher at higher $[Ca^{2+}]_o$, but this is at least partially explained by variations in cell density: the number of cells counted 2 d after medium change was decreased in lower $[Ca^{2+}]_o$ and increased in higher $[Ca^{2+}]_o$ (Fig. 5F). Amplitudes were not significantly different in all concentrations (Fig. 5C). Circadian periods were significantly shorter at lower $[Ca^{2+}]_o$ [23.7 ± 0.46 h (mean ± SE) in 0 mM Ca^{2+} with 10 μM EGTA, n = 3; 24.2 ± 0.16 h in 0 mM Ca^{2+}, n = 6; 25.6 ± 0.12 h in control, $p < 0.01$, *ANOVA* followed by Dunnett's test] (Fig. 5D). Also, phases were advanced at lower $[Ca^{2+}]_o$, reflecting the shorter periods (Fig. 5E).

Buffering $[Ca^{2+}]_i$ and blocking release from intracellular Ca^{2+} stores delay phases of fibroblast PER2::LUC rhythms

Preventing Ca^{2+} influx by removing $[Ca^{2+}]_o$ caused shorter periods and advanced phases. These results did not resemble the effects of membrane hyperpolarization caused by removing $[K^+]_o$, which caused arrhythmicity or delayed phases. This pattern of results suggests that extracellular Ca^{2+} influx may not mediate effects of membrane potential on clock gene expression rhythms. We therefore hypothesized that effects of membrane potential manipulations may be conveyed by cytosolic Ca^{2+}, or Ca^{2+} release from intracellular Ca^{2+} stores. To investigate effects of Ca^{2+} from different sources on PER2 rhythmicity, we added to fibroblast cultures: BAPTA-AM (a chelator of intracellular Ca^{2+}), thapsigargin (a blocker of Ca^{2+} release from IP_3-sensitive intracellular stores), ryanodine (a blocker of Ca^{2+} release from ryanodine-sensitive intracellular stores), or nimodipine (a blocker of Ca^{2+} influx through plasma membrane L-type Ca^{2+} channels). Buffering $[Ca^{2+}]_i$ with 25 μM BAPTA-AM significantly lengthened period and delayed phase (Fig. 6A, H). Average brightness was not different from 0.1% DMSO in HMM control (Fig. 6E). Blocking release from intracellular Ca^{2+} stores by 10 nM thapsigargin significantly decreased brightness and delayed phases (Fig. 6B, E, H). Brightness recovered after changing medium to control medium (data not shown). Period and amplitude were not affected (Fig. 6F–G). Ryanodine activates Ca^{2+} release from ryanodine-sensitive stores at

lower concentrations and inhibits Ca^{2+} release at concentrations > 10 μM (Meissner, 1986). Ryanodine had no significant effect at 5 μM and delayed phases slightly at 200 μM (Fig. 6C, H). Nimodipine delayed phases slightly, but did not affect other circadian parameters (Fig. 6D, E–H).

Discussion

SCN neurons generate circadian rhythms of spontaneous neuronal firing, which depend on rhythms of resting membrane potential, but there is evidence that the transcription-based core feedback loop of the clock itself also depends on membrane potential (Colwell, 2011). For example, decreasing $[K^+]_o$ stops rhythmic *per1* transcription in mammalian SCN neurons (Lundkvist et al., 2005). This effect was confirmed in our results (Fig. 1B). Similarly, in *Drosophila*, hyperpolarizing circadian pacemaker neurons by overexpressing K^+ channels abolishes rhythms of clock gene expression (Nitabach et al., 2002). Our experiments extend these observations from pacemaker neurons to peripheral fibroblasts. Our data show that (1) decreasing $[K^+]_o$ delays or stops PER2::LUC rhythms of fibroblasts, (2) 0 mM $[K^+]_o$ abolishes individual fibroblast rhythms, (3) decreasing $[Ca^{2+}]_o$ shortens period and advances phase of fibroblast rhythms, and (4) buffering $[Ca^{2+}]_i$ lengthens period or delays phase.

There has been little work to date on the possible role of membrane electrical events in fibroblasts. In SCN neurons, several K^+ currents, including the fast delayed rectifier (FDR) K^+ current, the A-type K^+ current, and the large-conductance Ca^{2+}-activated K^+ current (BK), have been implicated in the regulation of spontaneous action potential firing during the day (Colwell, 2011; Itri et al., 2010; Meredith et al., 2006; Rudy & McBain, 2001). In human dermal fibroblasts, presence of voltage-gated K^+ channels, large-conductance Ca^{2+}-activated K^+ channels, and inward rectifier K^+ channels, have been demonstrated using patch-clamp techniques (Estacion, 1991). Furthermore, a microarray analysis found that the potassium channel regulatory protein, Na-K-Cl cotransporter, and L-type voltage-dependent calcium channel are rhythmically expressed in Rat-1 fibroblasts (Grundschober et al., 2001). Whether ion channels play a role in circadian clock function in non-neuronal cells as they do in SCN neurons has not been studied extensively, although Lundkvist et al. found that decreasing $[Ca^{2+}]_o$ stops rhythmic *per1* transcription in liver explants as well as in SCN slices (Lundkvist et al., 2005).

Reducing $[K^+]_o$ causes membrane hyperpolarization in fibroblasts in short term experiments (Baxter et al., 2002; Chilton et al., 2005; Yen-Chow et al., 1984), and it is likely that qualitatively similar effects apply in our cells. Attempts to measure membrane potential quantitatively in our cells by patch clamp recording were unsuccessful due to the technical challenges of patching very flat cells. Moreover, precise theoretical estimates based on Nernst equation calculations are likely to be misleading due to homeostatic compensation in long-term experiments.

In any event, we reduced $[K^+]_o$ to test the effects of membrane potential on PER2 rhythms in fibroblasts. The fibroblasts tolerated even nominally zero $[K^+]_o$, and on return to regular medium actually recovered rhythmicity with even higher amplitude than in control conditions (Fig. 3). Removing $[K^+]_o$ led to arrhythmic PER2 expression at the single cell level. We cannot exclude the possibility that circadian rhythms of other clock genes such as *Bmal1* or non-transcriptional oscillations such as redox cycles (O'Neill & Reddy, 2011) persist under this condition. However, given this dramatic effect on PER2 rhythms, it is clear that membrane potential plays an important role in maintaining the core circadian transcriptional-translational feedback loop. One possibility is that a circadian rhythm in membrane potential exists in fibroblasts and drives or reinforces clock gene rhythms (M. H.

Hastings et al., 2008). Alternatively, it may be that a minimum level of membrane potential is required for rhythmic activation of clock gene transcription in fibroblasts.

In the SCN, neuronal firing or membrane depolarization is known to be required for rhythmic expression of clock genes (Yamaguchi et al., 2003), and Ca^{2+} is a likely mediator of this process. Action potentials in the SCN neuron induce a rise in somatic calcium levels through L-type calcium channels (Irwin & Allen, 2007). Lowering $[Ca^{2+}]_o$ or blocking voltage-dependent Ca^{2+} channels abolishes the rhythmic expression of *Per1* in rat SCN and liver explants (Lundkvist et al., 2005), and we found similar effects on *Per2* expression in mouse SCN (Fig. 1C). These studies suggest the importance of transmembrane Ca^{2+} flux for circadian clock function.

Interestingly, however, SCN neurons have a rhythmically regulated intracellular pool of Ca^{2+} (Ikeda et al., 2003). It is not known whether the circadian rhythms of $[Ca^{2+}]_i$ observed in SCN neurons also occur in fibroblasts. These Ca^{2+} rhythms in SCN neurons are sensitive to pharmacological manipulation of ryanodine-sensitive stores of intracellular Ca^{2+} but not to TTX or L-type Ca^{2+} channel blockers. Manipulating $[Ca^{2+}]_i$ also strongly affects circadian rhythms of pacemaker neurons. Blocking release from intracellular Ca^{2+} stores abolishes neuronal firing in the SCN (Ikeda et al., 2003). Buffering $[Ca^{2+}]_i$ with BAPTA-AM stops rhythmic expression of *Per1* in the SCN (Lundkvist et al., 2005), and we found similar effects on *Per2* expression in mouse SCN (Fig. 1D). Similarly, in *Drosophila*, buffering $[Ca^{2+}]_i$ in pacemaker neurons results in dose-dependent slowing of free-running behavioral and molecular rhythms (Harrisingh et al., 2007). These results indicate the importance of intracellular Ca^{2+} as well as Ca^{2+} influx from outside the cell in pacemaker neurons.

In fibroblasts, it has been shown that depolarization caused by high $[K^+]_o$ induces Ca^{2+} influx (Etcheberrigaray et al., 1993), so it is plausible that effects of membrane potential manipulations on the fibroblast clock could be mediated through Ca^{2+} influx. In the present study, fibroblasts did not lose rhythmicity in medium with any external Ca^{2+} concentration tested (0 mM < $[Ca^{2+}]_o$ < 14.4 mM), unlike SCN slices (compare Figs. 1C vs. 5A). In SCN slices, lowering $[Ca^{2+}]_o$ may disrupt both communication between neurons through neurotransmitters and cell autonomous rhythms, whereas in fibroblast cultures there is no intercellular circadian communication to be disrupted (Nagoshi et al., 2004; Welsh et al., 2004). Ca^{2+} signaling may have a more prominent role in SCN neurons than in non-neuronal cells by enhancing rhythm coupling among cells in neuronal circuits. In future studies, it will be important to clarify the precise relationship between membrane potential and $[Ca^{2+}]_i$ in long-term experiments, using genetically encoded Ca^{2+} indicators such as cameleon (Ikeda et al., 2003).

At lower $[Ca^{2+}]_o$, fibroblasts showed shorter periods, advanced phases, and persistent rhythms, in contrast to the delays and arrhythmicity induced by lowering $[K^+]_o$. On the other hand, buffering $[Ca^{2+}]_i$ by BAPTA-AM or manipulating IP_3-sensitive intracellular Ca^{2+} stores by thapsigargin resulted in longer period and delayed phases, similar to the effects of lowering $[K^+]_o$, although they did not abolish rhythmicity as seen in low $[K^+]_o$. This period lengthening caused by buffering $[Ca^{2+}]_i$ is consistent with results shown in *Drosophila* pacemaker neurons (Harrisingh et al., 2007). Our manipulations of $[Ca^{2+}]_i$ and $[Ca^{2+}]_o$ affected circadian rhythms of PER2 expression differently. In dorsal root ganglion neurons, it was shown that when $[Ca^{2+}]_o$ is lowered, Ca^{2+} is released from intracellular stores to maintain a constant $[Ca^{2+}]_i$ level for at least 1 h (Cohen & Fields, 2006). The release of Ca^{2+} from endoplasmic reticulum is linked to the influx of Ca^{2+} through plasma membrane channels. This coupling is well known as SOCE (store-operated Ca^{2+} entry) (Shen et al., 2011). In our experiments, it is possible that intracellular calcium stores maintained $[Ca^{2+}]_i$

at a constant level despite $[Ca^{2+}]_o$ depletion and that this refill of $[Ca^{2+}]_i$ caused different effects on circadian rhythms than actual buffering of $[Ca^{2+}]_i$. Also, it is possible that cell density might have mediated the effects of $[Ca^{2+}]_o$, as we observed that cell density varied with $[Ca^{2+}]_o$ (Fig. 5F).

Because membrane hyperpolarization and buffering $[Ca^{2+}]_i$, produced similar effects on rhythms, our data implicate intracellular Ca^{2+}, especially IP_3-sensitive Ca^{2+} stores, rather than a transmembrane Ca^{2+} flux, in the pathway that connects membrane potential to clock gene expression in fibroblasts. Changes in $[Ca^{2+}]_i$ may modulate CREB (cyclic AMP-responsive element (CRE)-binding protein) activity and control clock gene expression in fibroblasts (Pulivarthy et al., 2007), as in SCN neurons (Colwell, 2011). In future studies, it will be important to validate the well-established short-term effects of BAPTA-AM, thapsigargin, and ryanodine for longer experimental durations using genetically encoded, compartment-specific Ca^{2+} reporters (Ikeda et al., 2003).

Our findings provide evidence for a more generalized and fundamental importance of membrane electrical phenomena and intracellular Ca^{2+} in the function of cellular circadian clocks that is not unique to SCN neurons. These results support the concept of a pacemaker extending beyond a simple transcriptional feedback loop to a more integrated system involving electrical membrane events and Ca^{2+}-mediated cytoplasmic signaling, as well as cAMP (O'Neill et al., 2008). Because clock function involves such central cellular signaling pathways, not just in the SCN neuron but in other cells as well, the circadian clock can now be seen as a fundamental and inextricable aspect of mammalian cell physiology. Further studies of circadian rhythms in membrane potential and intracellular Ca^{2+} in fibroblasts will be required to understand the nature of this integrated cellular circadian clock.

Acknowledgments

Supported by NIH (R01 MH082945 to DKW) and a V.A. Career Development Award (DKW). We thank Lexie Wang for excellent research assistance, Dr. Gabriella Lundkvist for providing details of her experimental protocol, and Drs. Andrea Meredith and Michael McCarthy for helpful discussions. We also thank Dr. Meredith for attempted patch clamp experiments.

References

Baxter DF, Kirk M, Garcia AF, Raimondi A, Holmqvist MH, Flint KK, Bojanic D, Distefano PS, Curtis R, Xie Y. A novel membrane potential-sensitive fluorescent dye improves cell-based assays for ion channels. J Biomol Screen. 2002; 7:79–85. [PubMed: 11897058]

Bouskila Y, Dudek FE. A rapidly activating type of outward rectifier K+ current and A-current in rat suprachiasmatic nucleus neurones. J Physiol. 1995; 488(Pt 2):339–350. [PubMed: 8568674]

Chilton L, Ohya S, Freed D, George E, Drobic V, Shibukawa Y, Maccannell KA, Imaizumi Y, Clark RB, Dixon IM, Giles WR. K+ currents regulate the resting membrane potential, proliferation, and contractile responses in ventricular fibroblasts and myofibroblasts. Am J Physiol Heart Circ Physiol. 2005; 288:H2931–2939. [PubMed: 15653752]

Cohen JE, Fields RD. CaMKII inactivation by extracellular Ca(2+) depletion in dorsal root ganglion neurons. Cell Calcium. 2006; 39:445–454. [PubMed: 16519936]

Colwell CS. Linking neural activity and molecular oscillations in the SCN. Nat Rev Neurosci. 2011; 12:553–569. [PubMed: 21886186]

Estacion M. Characterization of ion channels seen in subconfluent human dermal fibroblasts. J Physiol. 1991; 436:579–601. [PubMed: 1712040]

Etcheberrigaray R, Ito E, Oka K, Tofel-Grehl B, Gibson GE, Alkon DL. Potassium channel dysfunction in fibroblasts identifies patients with Alzheimer disease. Proc Natl Acad Sci U S A. 1993; 90:8209–8213. [PubMed: 8367484]

Gee KR, Brown KA, Chen WN, Bishop-Stewart J, Gray D, Johnson I. Chemical and physiological characterization of fluo-4 Ca(2+)-indicator dyes. Cell Calcium. 2000; 27:97–106. [PubMed: 10756976]

Grundschober C, Delaunay F, Puhlhofer A, Triqueneaux G, Laudet V, Bartfai T, Nef P. Circadian regulation of diverse gene products revealed by mRNA expression profiling of synchronized fibroblasts. J Biol Chem. 2001; 276:46751–46758. [PubMed: 11598123]

Harrisingh MC, Wu Y, Lnenicka GA, Nitabach MN. Intracellular Ca2+ regulates free-running circadian clock oscillation in vivo. J Neurosci. 2007; 27:12489–12499. [PubMed: 18003827]

Hastings M, O'Neill JS, Maywood ES. Circadian clocks: regulators of endocrine and metabolic rhythms. J Endocrinol. 2007; 195:187–198. [PubMed: 17951531]

Hastings MH, Maywood ES, O'Neill JS. Cellular circadian pacemaking and the role of cytosolic rhythms. Curr Biol. 2008; 18:R805–R815. [PubMed: 18786386]

Ikeda M, Sugiyama T, Wallace CS, Gompf HS, Yoshioka T, Miyawaki A, Allen CN. Circadian dynamics of cytosolic and nuclear Ca2+ in single suprachiasmatic nucleus neurons. Neuron. 2003; 38:253–263. [PubMed: 12718859]

Irwin RP, Allen CN. Calcium response to retinohypothalamic tract synaptic transmission in suprachiasmatic nucleus neurons. J Neurosci. 2007; 27:11748–11757. [PubMed: 17959816]

Itri JN, Vosko AM, Schroeder A, Dragich JM, Michel S, Colwell CS. Circadian regulation of a-type potassium currents in the suprachiasmatic nucleus. J Neurophysiol. 2010; 103:632–640. [PubMed: 19939959]

Ko CH, Yamada YR, Welsh DK, Buhr ED, Liu AC, Zhang EE, Ralph MR, Kay SA, Forger DB, Takahashi JS. Emergence of noise-induced oscillations in the central circadian pacemaker. PLoS Biol. 2010; 8:e1000513. [PubMed: 20967239]

Kuhlman SJ, McMahon DG. Rhythmic regulation of membrane potential and potassium current persists in SCN neurons in the absence of environmental input. Eur J Neurosci. 2004; 20:1113–1117. [PubMed: 15305881]

Liu AC, Welsh DK, Ko CH, Tran HG, Zhang EE, Priest AA, Buhr ED, Singer O, Meeker K, Verma IM, Doyle FJ 3rd, Takahashi JS, Kay SA. Intercellular coupling confers robustness against mutations in the SCN circadian clock network. Cell. 2007; 129:605–616. [PubMed: 17482552]

Lundkvist GB, Kwak Y, Davis EK, Tei H, Block GD. A calcium flux is required for circadian rhythm generation in mammalian pacemaker neurons. Journal of Neuroscience. 2005; 25:7682–7686. [PubMed: 16107654]

Meredith AL, Wiler SW, Miller BH, Takahashi JS, Fodor AA, Ruby NF, Aldrich RW. BK calcium-activated potassium channels regulate circadian behavioral rhythms and pacemaker output. Nat Neurosci. 2006; 9:1041–1049. [PubMed: 16845385]

Mohawk JA, Takahashi JS. Cell autonomy and synchrony of suprachiasmatic nucleus circadian oscillators. Trends Neurosci. 2011

Nagoshi E, Saini C, Bauer C, Laroche T, Naef F, Schibler U. Circadian gene expression in individual fibroblasts: cell-autonomous and self-sustained oscillators pass time to daughter cells. Cell. 2004; 119:693–705. [PubMed: 15550250]

Nakamura W, Yamazaki S, Nakamura TJ, Shirakawa T, Block GD, Takumi T. In vivo monitoring of circadian timing in freely moving mice. Curr Biol. 2008; 18:381–385. [PubMed: 18334203]

Nitabach MN, Blau J, Holmes TC. Electrical silencing of Drosophila pacemaker neurons stops the free-running circadian clock. Cell. 2002; 109:485–495. [PubMed: 12086605]

O'Neill JS, Maywood ES, Chesham JE, Takahashi JS, Hastings MH. cAMP-dependent signaling as a core component of the mammalian circadian pacemaker. Science. 2008; 320:949–953. [PubMed: 18487196]

O'Neill JS, Reddy AB. Circadian clocks in human red blood cells. Nature. 2011; 469:498–503. [PubMed: 21270888]

Portaluppi F, Smolensky MH, Touitou Y. Ethics and methods for biological rhythm research on animals and human beings. Chronobiol Int. 2010; 27:1911–1929. [PubMed: 20969531]

Pulivarthy SR, Tanaka N, Welsh DK, De Haro L, Verma IM, Panda S. Reciprocity between phase shifts and amplitude changes in the mammalian circadian clock. Proc Natl Acad Sci U S A. 2007; 104:20356–20361. [PubMed: 18077393]

Rudy B, McBain CJ. Kv3 channels: voltage-gated K+ channels designed for high-frequency repetitive firing. Trends Neurosci. 2001; 24:517–526. [PubMed: 11506885]

Shen WW, Frieden M, Demaurex N. Remodelling of the endoplasmic reticulum during store-operated calcium entry. Biol Cell. 2011; 103:365–380. [PubMed: 21736554]

Welsh DK, Imaizumi T, Kay SA. Real-time reporting of circadian-regulated gene expression by luciferase imaging in plants and mammalian cells. Methods Enzymol. 2005; 393:269–288. [PubMed: 15817294]

Welsh DK, Logothetis DE, Meister M, Reppert SM. Individual neurons dissociated from rat suprachiasmatic nucleus express independently phased circadian firing rhythms. Neuron. 1995; 14:697–706. [PubMed: 7718233]

Welsh, DK.; Noguchi, T. Cellular bioluminescence imaging. In: Yuste, R., editor. Imaging: A Laboratory Manual. Cold Spring Harbor, NY: Cold Spring Harbor Laboratory Press; 2011. p. 369-385.

Welsh DK, Takahashi JS, Kay SA. Suprachiasmatic nucleus: cell autonomy and network properties. Annu Rev Physiol. 2010; 72:551–577. [PubMed: 20148688]

Welsh DK, Yoo SH, Liu AC, Takahashi JS, Kay SA. Bioluminescence imaging of individual fibroblasts reveals persistent, independently phased circadian rhythms of clock gene expression. Curr Biol. 2004; 14:2289–2295. [PubMed: 15620658]

Yamaguchi S, Isejima H, Matsuo T, Okura R, Yagita K, Kobayashi M, Okamura H. Synchronization of cellular clocks in the suprachiasmatic nucleus. Science. 2003; 302:1408–1412. [PubMed: 14631044]

Yen-Chow YC, Chow SY, Jee WS, Woodbury DM. Membrane potentials, electrolyte contents, cell pH, and some enzyme activities of fibroblasts. In Vitro. 1984; 20:677–684. [PubMed: 6238900]

Yoo SH, Yamazaki S, Lowrey PL, Shimomura K, Ko CH, Buhr ED, Siepka SM, Hong HK, Oh WJ, Yoo OJ, Menaker M, Takahashi JS. PERIOD2::LUCIFERASE real-time reporting of circadian dynamics reveals persistent circadian oscillations in mouse peripheral tissues. Proc Natl Acad Sci U S A. 2004; 101:5339–5346. [PubMed: 14963227]

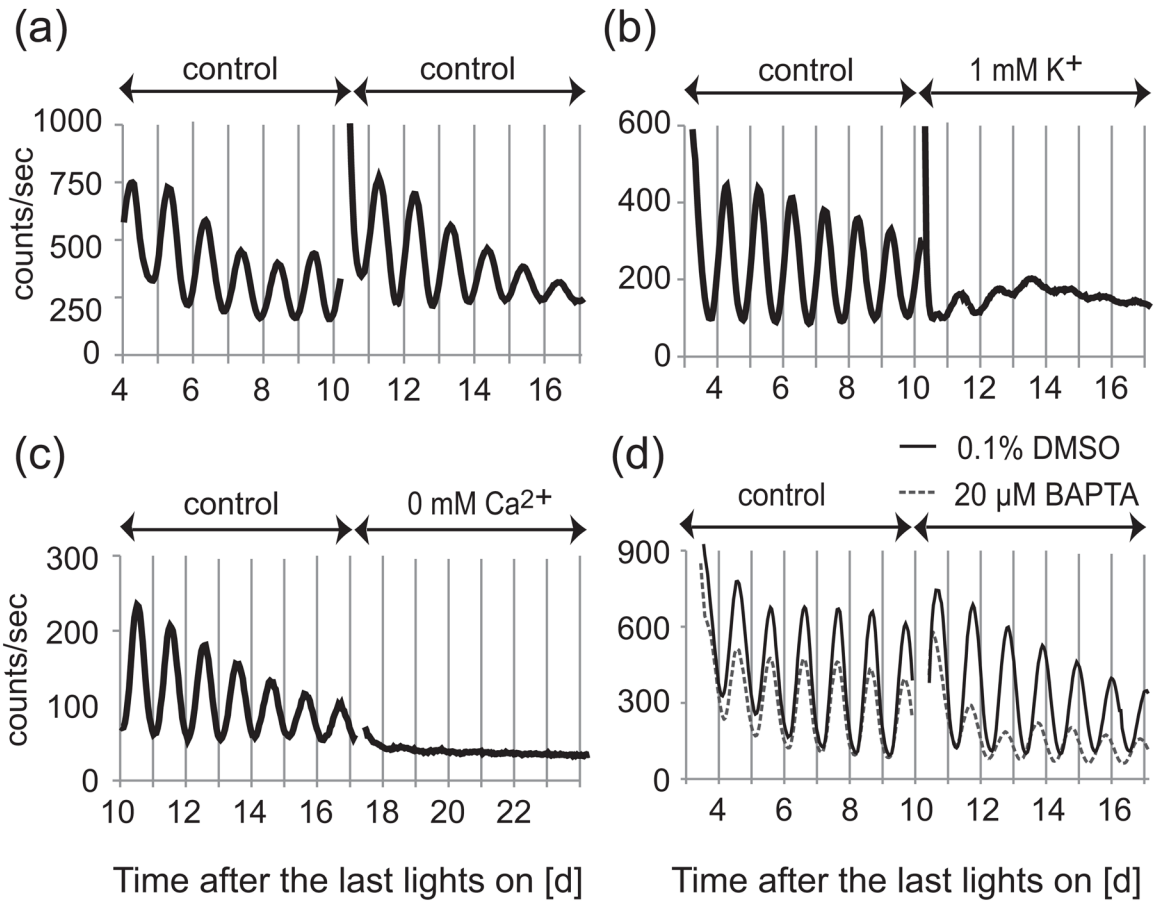

Figure 1.

Representative recordings of PER2::LUC bioluminescence from SCN slices cultured in control medium, low K^+, low Ca^{2+}, or Ca^{2+} chelator. SCN slices were cultured in HMM control medium for 1–2 weeks and then transferred to fresh HMM control medium (A), or medium with 1 mM K^+ (B), 1 mM Ca^{2+} (C), or 40 μM BAPTA-AM (D). In the case of BAPTA-AM (dissolved in 0.1% DMSO), control medium also contains 0.1% DMSO.

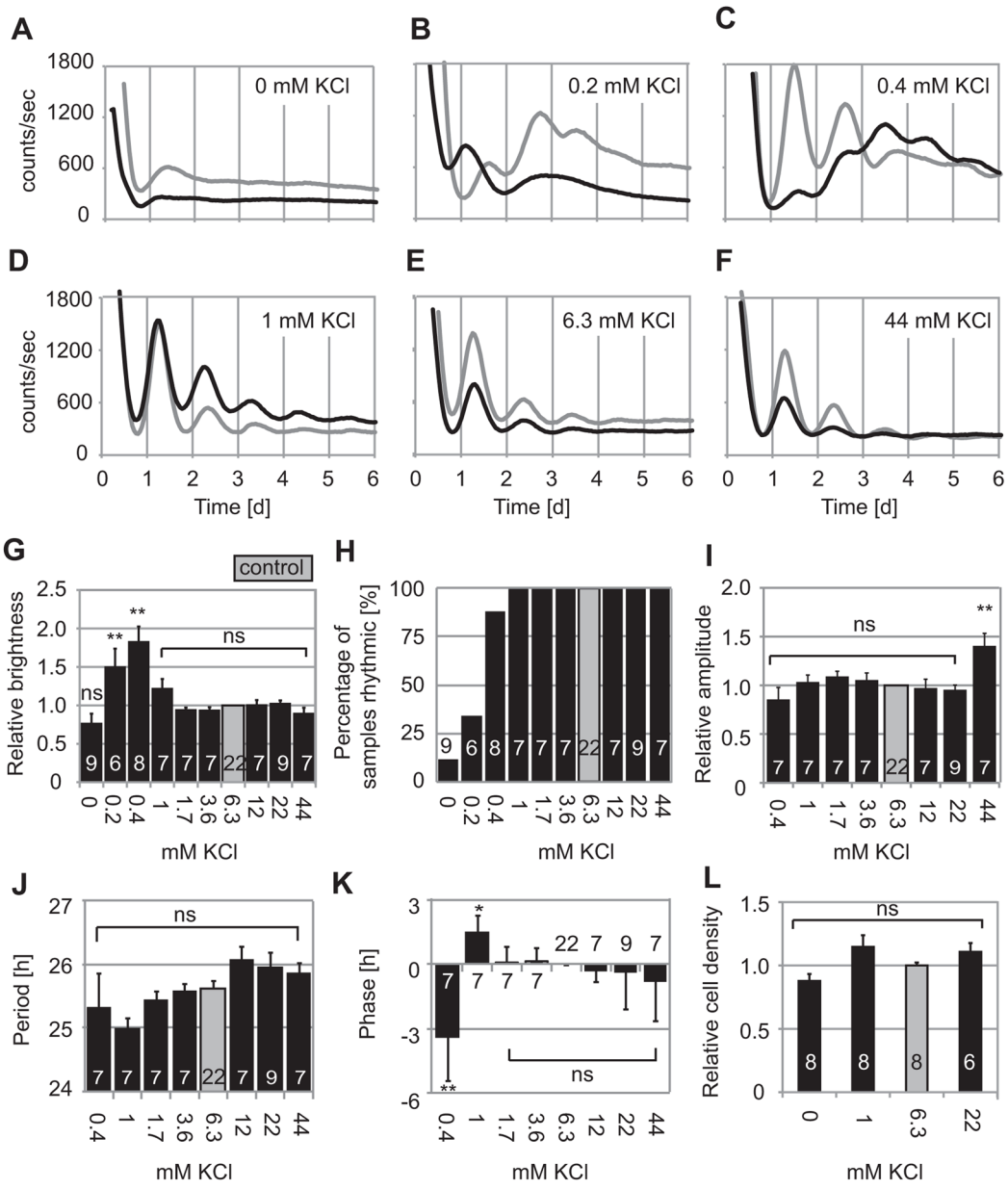

Figure 2.

Rhythms of fibroblasts cultured in various K^+ concentrations. Two representative PER2::LUC bioluminescence recordings are shown of fibroblast cultures in HMM with 0 (A), 0.2 (B), 0.4 (C), 1 (D), 6.3 (E), or 44 (F) mM K^+. Fibroblasts showed clear circadian rhythms in 1–44 mM K^+ (D – F), but generally showed poor or no rhythms in 0–0.2 mM K^+ (A – C). Data represented by black lines were collected simultaneously in parallel experiments. (G) Brightness relative to 6.3 mM K^+ control (gray). (H) Percentage of samples in each condition judged rhythmic by spectral analysis. Amplitudes (I), periods (J), and phases (K) relative to control, for samples categorized as rhythmic. (L) Cell density relative to control cultures. Columns show average values ± SE. Number of cultures in each condition are indicated by white numerals within columns. ns, not significant; $*p < 0.05$, $**p < 0.01$ compared to control (*ANOVA* followed by Dunnett's test).

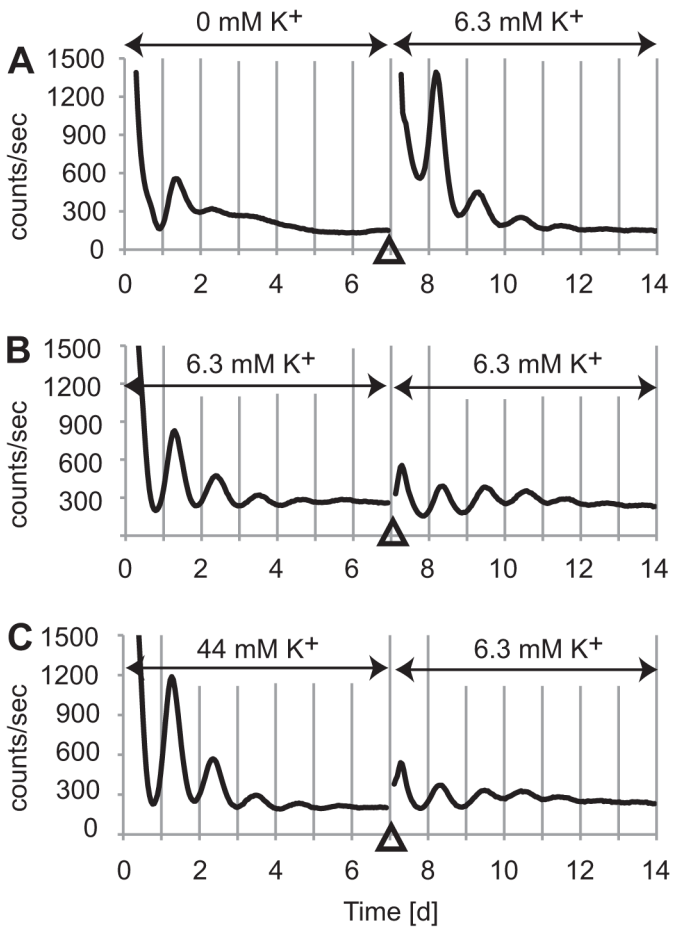

Figure 3.

Fibroblasts recovered clear circadian rhythmicity after medium change to HMM control. Medium was changed from 0 mM (A), 6.3 mM (B), or 44 mM (C) K^+ to 6.3 mM K^+ control at 7th day in culture. *X*-axis shows time after medium change. *Y*-axis shows relative bioluminescence intensity [counts/sec].

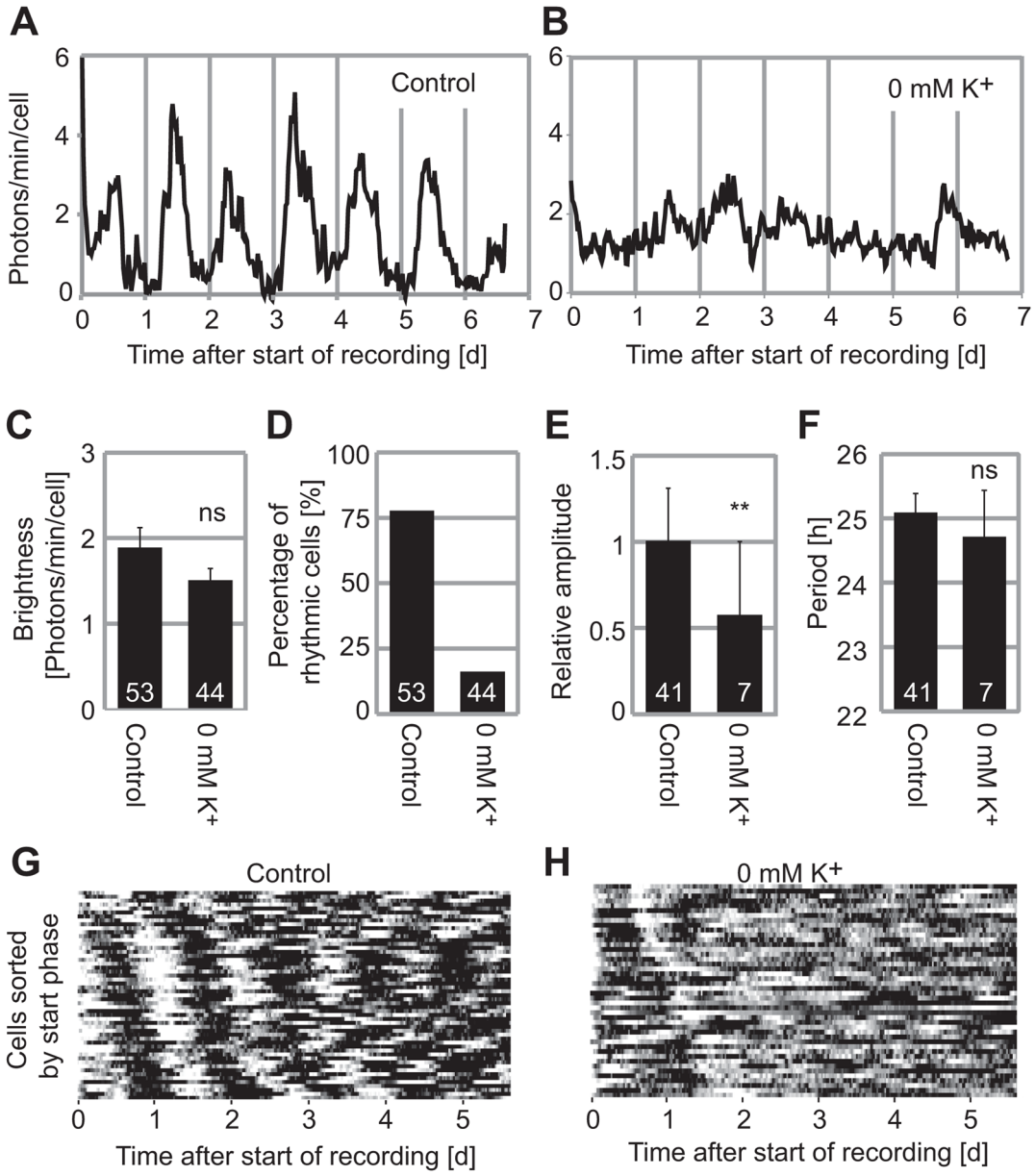

Figure 4.

Fibroblasts in 0 mM K^+ lose rhythmicity at the single cell level. Fibroblasts were cultured in control medium (A) and in 0 mM K^+ (B) for 7 d. *X*-axis shows time after start of recording and *Y*-axis show photons/min/cell. (C) Average brightness of single cells. Brightness was not significantly different in 0 mM K^+ compared to control (Student's *t*-test, ns; $p > 0.05$). (D) Percentage of single cells in each condition judged rhythmic by spectral analysis. (E) Amplitudes of rhythmic cells, relative to control (Student's *t*-test, **; $p < 0.01$). (F) Periods of rhythmic cells. There was no significant difference from control (Student's *t*-test, $p > 0.05$). Columns show average values ± SE. Numbers of cells in each condition are indicated by white numerals within columns. Bioluminescence rhythms of all 53 fibroblasts from 5 experiments (G) and 44 fibroblasts from 3 experiments (H) are represented in raster plots. Each horizontal raster line represents a single cell, with elapsed time plotted left to right. Bioluminescence intensity data from all cells were normalized for average brightness and

then color-coded: higher than average values are white, and lower than average values are black. The cells are sorted in order of start phase, so that emergence of desynchrony can be more easily appreciated.

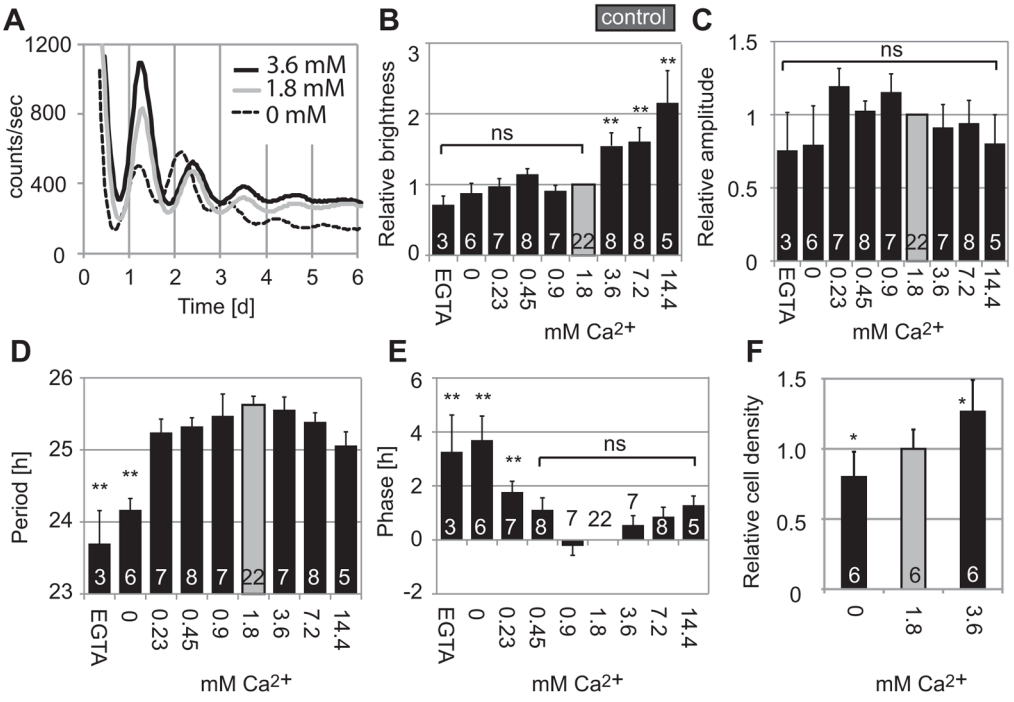

Figure 5.

Representative recordings of PER2::LUC bioluminescence from fibroblast cultures in various Ca^{2+} concentrations (A). Fibroblasts were cultured in HMM with 0 (dashed line), 1.8 (control, gray line), or 3.6 mM Ca^{2+} (black line). Fibroblasts showed clear circadian rhythms in all cases. (B) Brightness relative to 1.8 mM Ca^{2+} control. Amplitudes relative to control (C), periods (D), and phases (E) of samples categorized as rhythmic. Fibroblasts were increased in number in HMM with 3.6 mM Ca^{2+} and decreased in 0 mM Ca^{2+} (F). Columns show average values ± SE. Numbers of cultures are indicated by white numerals within columns. ns, not significant; $*p < 0.05$, $**p < 0.01$ compared to control (*ANOVA* followed by Dunnett's test).

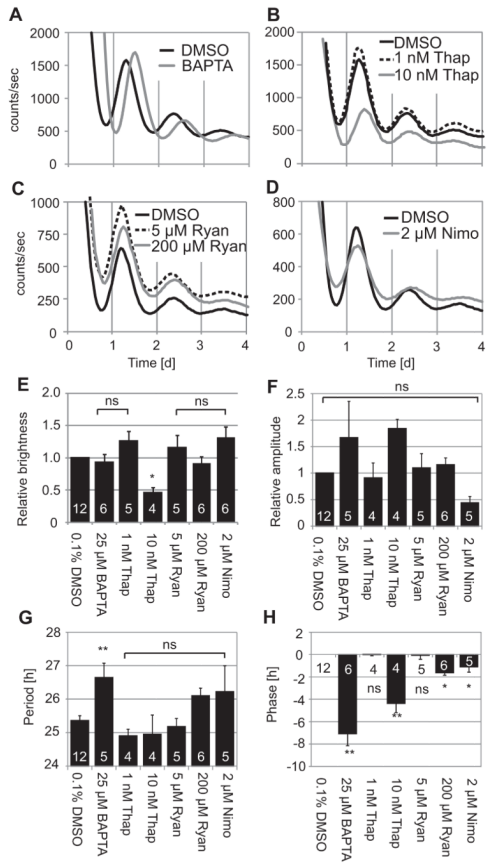

Figure 6.

(A – D) Representative recordings of PER2::LUC bioluminescence from fibroblasts cultured in various Ca^{2+} modulators. Fibroblasts were cultured in control HMM with 0.1% DMSO, 25 μM BAPTA-AM (A), 1 or 10 nM thapsigargin (B), 5 or 200 μM ryanodine (C), or 2 μM nimodipine (D). Fibroblasts showed clear circadian rhythms in all cases, except for one sample in 1 nM Thapsigargin and one sample in 2 μM nimodipine. Data in the same panels were collected simultaneously in parallel experiments. Column plots show brightness (E), rhythm amplitude (F), period (G), and phase (H) relative to control HMM. Bars show average values ± SE. Numbers of samples are indicated by white numerals within columns. ns, not significant; *$p < 0.05$, **$p < 0.01$ compared to control (*ANOVA* followed by Dunnett's test). BAPTA; BAPTA-AM, Thap: thapsigargin, Ryan; ryanodine, Nimo; nimodipine.

Table 1

Home Made Medium (HMM) Control Formuration	
Components	**Concentration [mM]**
Amino Acids	
Glycine	0.4
L-Arginine hydrochloride	1.198
L-Cystine	0.2
L-Glutamine	4
L-Histidine hydrochloride-H_2O	0.4
L-Isoleucine	0.8
L-Leucine	0.8
L-Lysine hydrochloride	0.7924
L-Methionine	0.2028
L-Phenylalanine	0.4
L-Serine	0.4
L-Threonine	0.8
L-Tryptophan	0.1
L-Tyrosine	0.3976
L-Valine	0.8
Vitamins	
Choline chloride	0.0286
D-Calcium pantothenate	0.00839
Folic Acid	0.00907
Nicotinamide	0.0328
Pyridoxal hydrochloride	0.0196
Riboflavin	0.00106
Thiamine hydrochloride	0.0119
i-Inositol	0.04

Home Made Medium (HMM) Control Formuration	
Components	**Concentration [mM]**
Inorganic Salts	
Calcium Chloride ($CaCl_2$) (anhyd.)	1.8
Potassium Chloride (KCl)	5.33
Sodium Chloride (NaCl)	116.11
Magnesium Sulfate ($MgSO_4$) (anhyd.)	0.814
Sodium Bicarbonate ($NaHCO_3$)	4.2
Sodium Phosphate monobasic (NaH_2PO_4-H_2O)	0.9075
Other Components	
D-Glucose (Dextrose)	24
HEPES	10
Pyruvic acid	1
D-Luciferin firefly, potassium salt	1
Penicillin	25 [U/ml]
Streptomycin	25 [mg/ml]
B-27 supplement 50x	2 [%]

Variable Components					
Medium	**$CaCl_2$ [mM]**	**KCl [mM]**	**NaCl [mM]**	**D-Luciferin potassium salt [mM]**	**D-Luciferin sodium salt [mM]**
Control (6.3 mM K^+ 1.8 mM Ca^{2+})	1.8	5.3	116	1	0
0 mM K^+	1.8	0.0	121	0	1
0.2 mM K^+	1.8	0.2	121	0	1
0.4 mM K^+	1.8	0.4	121	0	1
1.0 mM K^+	1.8	0.0	121	1	0
1.7 mM K^+	1.8	0.7	121	1	0
3.6 mM K^+	1.8	2.7	119	1	0
12 mM K^+	1.8	11.0	111	1	0

Variable Components					
Medium	**$CaCl_2$ [mM]**	**KCl [mM]**	**NaCl [mM]**	**D-Luciferin potassium salt [mM]**	**D-Luciferin sodium salt [mM]**
22 mM K^+	1.8	21.0	100	1	0
44 mM K^+	1.8	43.0	79	1	0
0 mM Ca^{2+}	0	5.3	118	1	0
0.23 mM Ca^{2+}	0.23	5.3	118	1	0
0.45 mM Ca^{2+}	0.45	5.3	117	1	0
0.9 mM Ca^{2+}	0.9	5.3	117	1	0
3.6 mM Ca^{2+}	3.6	5.3	114	1	0
7.2 mM Ca^{2+}	7.2	5.3	111	1	0
14.4 mM Ca^{2+}	14.4	5.3	104	1	0

* 10% volume dH_2O was added in all HMM medium to adjust osmolality.

* Removal or addition of KCl or $CaCl_2$ were compensated by NaCl

* Potassium salt from D-luciferin was added to potassium concentration.